XX Polish Fluid Mechanics Conference,
Gliwice, 17-20 September 2012

CAPTURING OF INTERFACE EVOLUTION USING DIFFUSE INTERFACE METHOD

Andrzej F. Nowakowski, Ahmed Ballil, Shaban A. Jolgam, Franck C. G. A. Nicolleau
Sheffield Fluid Mechanics Group, Mechanical Engineering Department,
University of Sheffield, Sheffield S1 3JD, United Kingdom.
E-mail: a.f.nowakowski@sheffield.ac.uk

Abstract

In the present contribution the diffuse interface method is used to track the interface evolution in multi-component flow systems. A numerical framework is developed to solve a hyperbolic Eulerian type model with a general stiffened gas equation of state. The model consists of six equations with two pressures and single velocity. The extended finite volume method is developed using a second order Godunov approach which is implemented with HLL and HLLC Riemann solvers in one and two space dimensions. The numerical scheme considers both the non-conservative equations and non-conservative terms that exist in the model to fulfill the interface condition. A verification procedure starts with a successful computation of a selection of numerical benchmark problems. Further, a numerically challenging shock bubble interaction problem is conducted and compared with published experimental data.

Key words: numerical simulations, compressible multi-component flow, interface evolution, shock waves, Riemann solver

INTRODUCTION

Multi-component flows with interface interactions and significant density variations occur in many industrial applications and physical phenomena. Good examples are cavitations, fuel injection and atomization systems. Using the numerical and experimental framework many attempts have been carried out to capture and track the interface evolution. For instance, the interaction of weak shock waves with cylindrical and spherical gas inhomogeneities is studied in (Hass and Sturtevant, 1987). The distortion of a spherical gaseous interface accelerated by a plane shock wave is monitored experimentally in (Layes *et al*., 2003). Quantitative numerical and experimental studies of the shock accelerated heterogeneous bubbles motion are made in (Layes and Le Métayer, 2007). The interaction of a shock wave with a rectangular block of sulphur hexafluoride (SF_6), occupying part of the test section of a shock tube, is studied by experimental and numerical means in (Bates *et al*., 2007). An efficient shock-capturing algorithm for compressible multi-component problems is developed by (Shyue, 1998). An interface capturing method for the simulation of multi-phase compressible flows is developed in (Shukla *et al*., 2010). Simulation of multiphase flows with strong shocks and density variations is carried out in (Nowakowski *et al.*, 2011).

The interface evolution problems could be addressed using different mathematical models and numerical methods. The technique classified as a diffuse interface method has been chosen in this study as an attractive option to mathematically represent and numerically simulate flows with interfaces. The method considers interfaces, for example contact discontinuities in gas dynamics, as numerically diffused zones taking advantage of inherent numerical diffusion. The formulation for the diffuse interface method was obtained after an

averaging process of the single phase Navier-Stokes equations. In this context various variants of mathematical models have been derived to represent flows with interfaces and subsequently many solution methods are proposed. For example: a model consisting of seven differential equations with two pressures and two velocities is proposed in (Saurel and Abgrall, 1999). This model has been considered as the most general and is known as the parent model. The model was numerically solved using a finite volume approach in (Saurel and Lemetayer, 2001). The numerical examples considered by these authors include calculations of water-air shock tube interactions, cavitations and detonation waves. Although the parent model does not need a mixture equation of state and provides thermodynamic variables for each phase, it is still computationally expensive and relatively complicated to implement as it needs to conduct both velocity and pressure relaxation processes during each step of time evolution. Some of these relaxation processes can be avoided if the parent model is used in a reduced form. Two similar reduced five equation models for simulation of compressible multi-component flows are proposed in (Allaire *et al*., 2000) and (Murrone and Guillard, 2005) respectively. Another model is derived in (Kapila *et al.*, 2001). In the latter reference a reduced Eulerian model is derived from the generic mathematical framework proposed by (Bear and Nunziato, 1986). The model consists of six equations in one dimensional space and has some significant advantages over the five equation models. These advantages concern the pressure equilibrium condition and are discussed in (Saurel *et al.*, 2009). The six equation model is further considered in this contribution and is subsequently used as a framework for developed numerical applications.

The paper considers a numerical approach for capturing and tracking the interface evolution. The thorough investigation of its performance is conducted based on existing benchmark numerical cases. Then the attempt to validate the approach is presented. The next two sections of the manuscript review the Eulerian mathematical model and summarize the developed numerical method. This is followed by numerical results and conclusions.

THE MULTIPHASE FLOW MODEL

The multiphase flow model considered in the present work was first derived by (Kapila *et al*., 2001) from the generic model of (Baer and Nunziato, 1986). The model consists of six differential equations that are two mass and two energy equations for each phase, one mixture momentum equation and the volume fraction evolution equation. This model is characterized by two pressures attributed to each phase and a single velocity. The model in one dimensional space can be expressed in the following form:

$$
\begin{aligned}
&\frac{\partial \alpha_g}{\partial t} + u\frac{\partial \alpha_g}{\partial x} = \mu\left(p_g - p_l\right),\\
&\frac{\partial \alpha_g \rho_g}{\partial t} + \frac{\partial \alpha_g \rho_g u}{\partial x} = 0,\\
&\frac{\partial \alpha_l \rho_l}{\partial t} + \frac{\partial \alpha_l \rho_l u}{\partial x} = 0,\\
&\frac{\partial \rho u}{\partial t} + \frac{\partial\left(\rho u^2 + p\right)}{\partial x} = 0,\\
&\frac{\partial \alpha_g \rho_g e_g}{\partial t} + \frac{\partial \alpha_g \rho_g e_g u}{\partial x} + \alpha_g p_g \frac{\partial u}{\partial x} = -\mu p_i\left(p_g - p_l\right),\\
&\frac{\partial \alpha_l \rho_l e_l}{\partial t} + \frac{\partial \alpha_l \rho_l e_l u}{\partial x} + \alpha_l p_l \frac{\partial u}{\partial x} = \mu p_i\left(p_g - p_l\right),
\end{aligned}
\tag{1}
$$

where α_k, ρ_k, u_k, p_k, e_k, ρ, u and p are the volume fraction, the density, the velocity, the pressure, the specific internal energy of the phase k, the mixture density, mixture velocity and mixture pressure, respectively. The subscript k refers to the subscripts g, l and i in the system (1) that denote gas, liquid and interface, respectively. In order to circumvent the difficulties related to the model's mechanical equilibrium and to maintain the volume fraction positivity, the model contains an additional total mixture energy equation which was derived in (Saurel *et al.*, 2009). This equation is obtained from summing up the two internal energy equations with mass and momentum equations and takes the following final form:

$$\frac{\partial\left(\rho e+\frac{1}{2}\rho u^2\right)}{\partial t}+\frac{\partial u\left(\rho e+\frac{1}{2}\rho u^2+p\right)}{\partial x}=0, \tag{2}$$

where ρe is the mixture internal energy which may be defined as

$$\rho e=\alpha_g\rho_g e_g+\alpha_l\rho_l e_l. \tag{3}$$

The characteristic feature of this multiphase flow model is the presence of separate pressure fields associated with each phase which are subjected to the pressure relaxation procedures. The terms in the right hand side of the model (1) are needed in the relaxation process to draw the non-equilibrium pressures to the equilibrium state. The μ variable represents a homogenization parameter controlling the rate at which pressure tends towards equilibrium. Its physical meaning has been justified using the second law of thermodynamics (Baer and Nunziato, 1986).

As there are still more unknown variables than equations in the model (1), there is a necessity to use the following relations to close the model:

- The constraint for total volume fraction of phases

$$\alpha_g+\alpha_l=1. \tag{4}$$

- The formula for the mixture velocity and the assumption that the interfacial pressure is equal to the mixture pressure

$$u=\frac{\alpha_g\rho_g u_g+\alpha_l\rho_l u_l}{\rho}, \qquad p_I=p=\alpha_g p_g+\alpha_l p_l, \tag{5}$$

  where the mixture density ρ is defined as

$$\rho=\alpha_g\rho_g+\alpha_l\rho_l. \tag{6}$$

- The equation of state (EOS) for each phase. The following stiffened gas equation of state can be used to govern both liquids and gases:

$$p=(\gamma-1)\rho e-\gamma\pi, \tag{7}$$

  where γ is a heat capacity ratio and π is a pressure constant depending on the fluid under consideration. The constant parameters are usually determined from experimental curves for each fluid.

NUMERICAL METHOD

The multiphase flow model (1) is hyperbolic but non-conservative i.e. cannot be written in the divergence form. Therefore the standard numerical methods developed for solving the hyperbolic conservation laws are not applicable directly. In order to solve the system (1) the numerical scheme is constructed, which decomposes governing equations into conservative (hyperbolic) and non-conservative source (relaxation) parts. Following the splitting technique introduced in (Strang, 1968), the numerical solution is obtained by consecutive operator steps on the conservative vector *U*. This takes a symbolic compact form:

$$U_i^{n+1} = L_s^{\Delta t/2} L_h^{\Delta t} L_s^{\Delta t/2} U_i^n , \tag{8}$$

where $L_h^{\Delta t}$ is the hyperbolic operator, $L_s^{\Delta t/2}$ is the source term operator U_i is the conservative vector at time level *n* and *n*+1.

The hyperbolic part of the model (1) can be rewritten in the quasi-linear formulation as

$$\begin{aligned} &\frac{\partial \alpha_g}{\partial t} + u_i \frac{\partial \alpha_g}{\partial x} = 0, \\ &\frac{\partial U}{\partial t} + \frac{\partial F(U)}{\partial x} = 0, \end{aligned} \tag{9}$$

where the conserved variables *U* and the fluxes $F(U)$ are given in a vector form as

$$U = \begin{bmatrix} \alpha_g \rho_g \\ \alpha_l \rho_l \\ \rho u \\ \rho E \end{bmatrix} \quad \text{and} \quad F(U) = \begin{bmatrix} \alpha_g \rho_g u \\ \alpha_l \rho_l u \\ \rho u^2 + \alpha\, p \\ u(\rho E + p) \end{bmatrix}. \tag{10}$$

The elements in the last row of the above vectors in (10) represent the additional equation of the total mixture energy (2). The hyperbolic part (9) is solved using a Godunov-type scheme. The explicit first-order Godunov scheme can be written as

$$U_i^{n+1} = U_i^n - \frac{\Delta t}{\Delta x}\left[F\left(U^*\left(U_i^n, U_{i+1}^n\right)\right) - F\left(U^*\left(U_{i-1}^n, U_i^n\right)\right)\right]. \tag{11}$$

The non-conservative equation for the volume fraction is discretised as follows

$$\alpha_i^{n+1} = \alpha_i^n - \frac{\Delta t}{\Delta x} u_i \left[(u\alpha_1)_{i+1/2}^* - (u\alpha_1)_{i-1/2}^* - \alpha_{1i}^n \left(u_{i+1/2}^* - u_{i-1/2}^*\right)\right]. \tag{12}$$

The non-conservative equation for the internal energy equation is discretised as follows:

$$(\alpha\rho e)_{ki}^{n+1} = (\alpha\rho e)_{ki}^n - \frac{\Delta t}{\Delta x} u_i \left[(\alpha\rho eu)_{ki+1/2}^* - (\alpha\rho eu)_{ki-1/2}^* - (\alpha p)_{ki}^n \left(u_{i+1/2}^* - u_{i-1/2}^*\right)\right]. \tag{13}$$

In the present work the second order accuracy is achieved using the MUSCL scheme described in (Toro, 2009). The robust and efficient HLL and HLLC approximate Riemann solvers for Euler equations are extended to calculate the numerical fluxes in the considered six-equation model.

In each time step once the first part of the solution algorithm representing the transport problem $L_h^{\Delta t}$ is accomplished, the pressure is modified by relaxation solver $L_s^{\Delta t/2}$. In this part of the solution procedure the differential equations containing the source terms of the original model (1) are:

$$\frac{\partial U}{\partial t} = \begin{bmatrix} \mu\left(p_g - p_l\right) \\ 0 \\ 0 \\ 0 \\ -\mu p_i\left(p_g - p_l\right) \\ \mu p_i\left(p_g - p_l\right) \\ 0 \end{bmatrix}, \tag{14}$$

where $U = \left[\alpha_g, \alpha_g\rho_g, \alpha_l\rho_l, \rho u, \alpha_g\rho_g e_g, \alpha_l\rho_l e_l, \rho E\right]^T$ The iterative relaxation method (procedure 4) given in (Lallemand et al. 2005) is utilized to perform direct integration of (14). The computed volume fraction together with the mixture energy ρe, which is calculated from the conservative total mixture energy equation (2), are used to obtain the mixture pressure from the mixture EOS. The mixture EOS is related to the stiffened EOS of each constituent as follows:

$$p = \frac{\rho e - \sum_k^2 \left(\frac{\alpha_k \gamma_k \pi_k}{\gamma_k - 1} \right)}{\sum_k^2 \left(\frac{\alpha_k}{\gamma_k - 1} \right)}. \tag{15}$$

TEST PROBLEMS AND RESULTS

The first two examples employed to test the numerical performance of the introduced approach are classical one dimensional multi-component benchmark flow problems. These cases enable the verification of the numerical algorithm using idealized analytical solutions. The considered two dimensional flow problems were: interface translation, underwater explosion and shock-bubble interaction. In all tests HLL and HLLC approximate Riemann solvers were used. The common assumption in all the conducted test problems is the presence of a negligible volume fraction 10^{-8} of the other fluid in the fluid considered as a pure fluid.

Water-air shock tube

This standard test problem is well documented in literature. For example, see (Ghangir and Nowakowski, 2012). The physical domain consists of a tube of 1 m length, which contains almost pure water at high pressure on the left hand side and air at atmospheric pressure on the right hand side. These constituents are separated by a diaphragm located at distance x = 0.7 m. The initial properties of both fluids are presented in Table 1. The computations were conducted using HLLC solver, a grid of 1000 computational cells and a CFL number equal to

0.6. The numerical results at time t = 229 μs show a very good agreement with the analytical solutions as shown in Figure 1. One can notice clearly a strong shock wave propagating from a high pressure liquid to a low pressure gas and rarefaction wave propagating in the opposite direction.

Table 1: Initial condition for water-air shock tube problem.

Physical property	Water	Air
Density, kg/m^3	1000	50
Velocity, m/s	0	0
Pressure, Pa	10^9	10^5
Heat capacity ratio (γ)	4.4	1.4
Pressure constant (π)	6×10^8	0

Interface interaction test

This test is described in (Hu and Khoo, 2004). It represents the interface interaction between two different gases with high pressure ratio. The length of the computational domain (tube) is 1 m with the initial diaphragm located at distance x = 0.2 m. Table 2 shows the initial conditions for both gases. The gas in the left chamber has an initial velocity and a higher pressure than the gas in the right chamber. Therefore, a shock wave propagates from left to right. The computation is made using HLL solver with a grid resolution of 1000 cells and a CFL = 0.6. The results obtained for the mixture velocity and mixture density are illustrated in Figure 2 at time t = 0.01 s associated with the exact solutions. Again a good agreement between both solutions can be noticed.

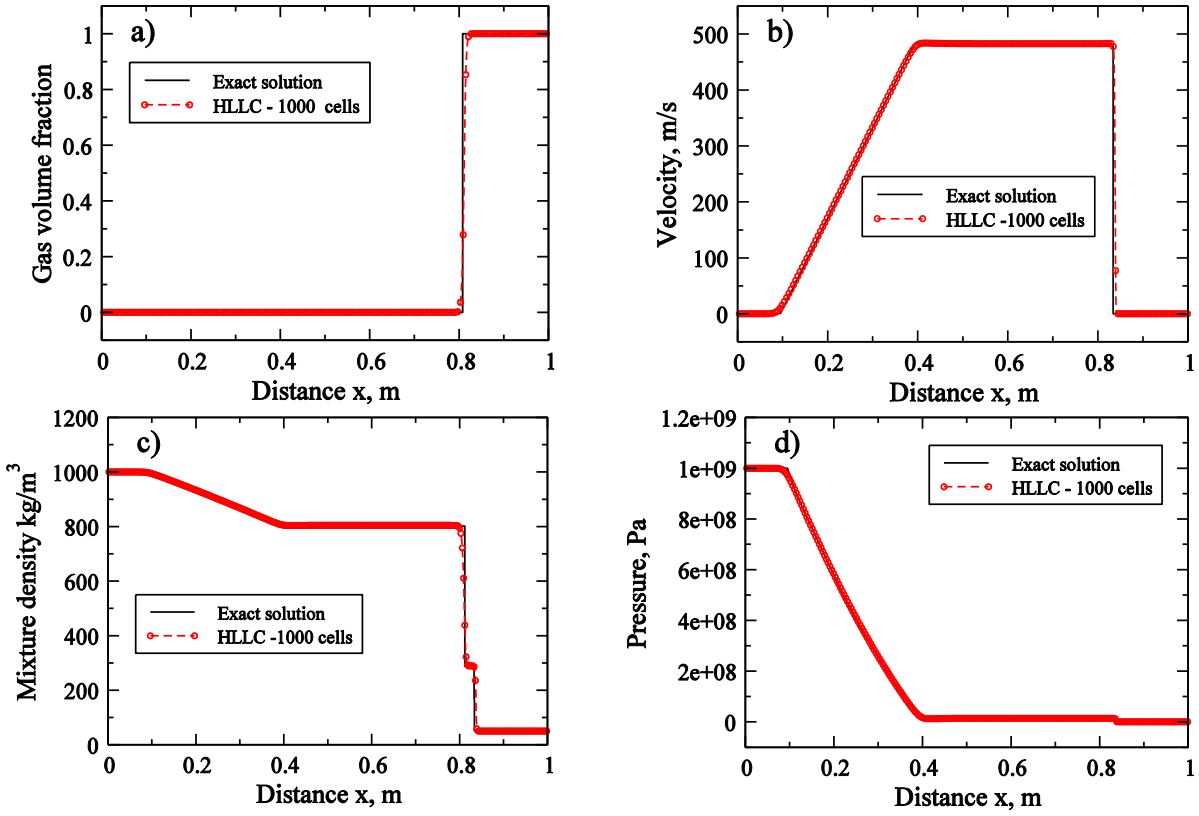

Fig. 1. Water-air shock tube at t = 229 μs: (a) Gas volume fraction, (b) Velocity, (c) Mixture density and (d) Pressure.

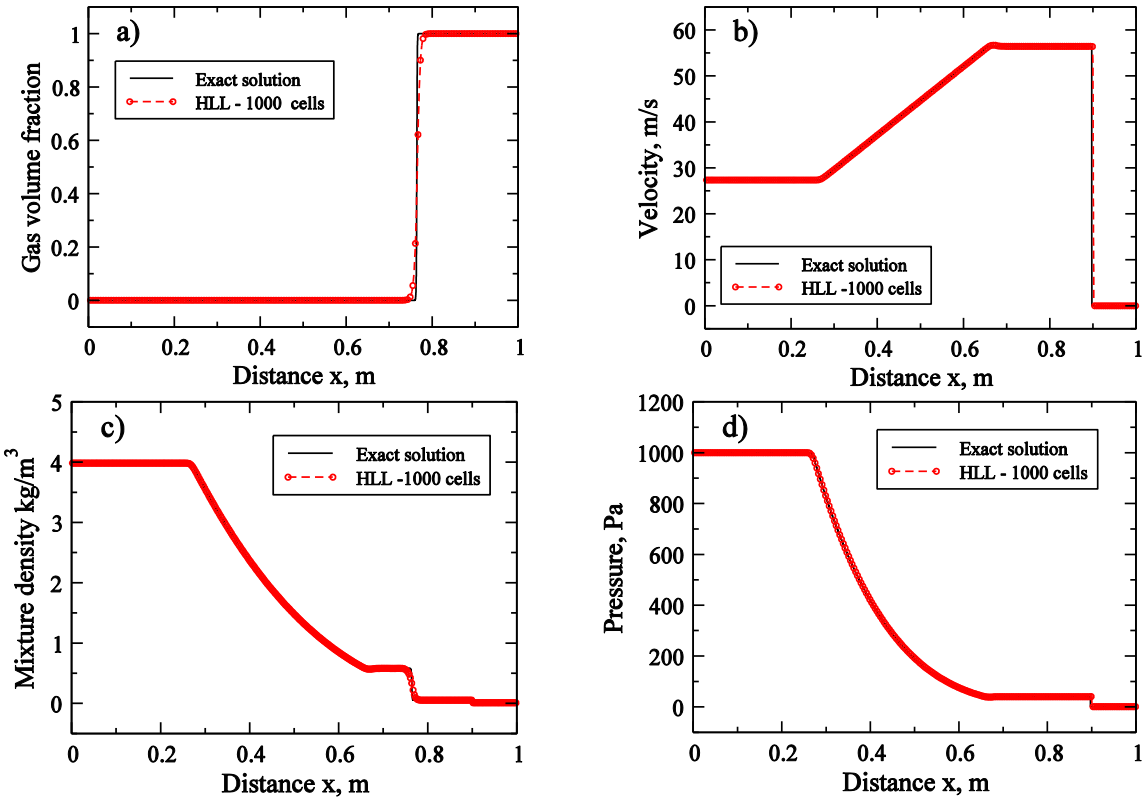

Fig. 2. Interface interaction test at t = 0.01 s: (a) Gas volume fraction, (b) Velocity, (c) Mixture density and (d) Pressure.

Table 2: Initial condition for interface interaction problem.

Physical property	Left chamber gas	Right chamber gas
Density, kg/m^3	3.984	0.01
Velocity, m/s	27.355	0
Pressure, Pa	1000	1
Heat capacity ratio (γ)	1.667	1.4
Pressure constant (π)	0	0

Unlike for the one dimensional test problems analytical solutions for the following two dimensional problems are not available. Therefore the simulated two-dimensional flows are verified against other numerical results generated using different models and numerical schemes.

Interface translation

The first two-dimensional test problem is the interface translation test. This test has been considered by many researchers, for example see (Shyue, 1998). Initially, a circular gas bubble with diameter d_o= 0.32 m is surrounded by another fluid in a square domain of 1×1 m. The location of the centre of the bubble is (0.25, 0.25) m and the initial conditions for both fluids are summarized in Table 3. In this computational task the HLLC Riemann solver with a grid resolution of 400×400 cells and a CFL = 0.3 is employed. Figure 3 shows the surface plots of the volume fraction at the initial time t = 0 s and time t = 0.36 s. The current results are consistent with those presented in (Shyue, 1998) and (Zheng, 2010).

Table 3: Initial condition for interface translation problem.

Physical property	Gas bubble	Surrounding fluid
Density, kg/m^3	1	0.1
Horizontal velocity, m/s	1	1
Vertical velocity, m/s	1	1
Pressure, Pa	1	1
Heat capacity ratio (γ)	1.4	1.6
Pressure constant (π)	0	0

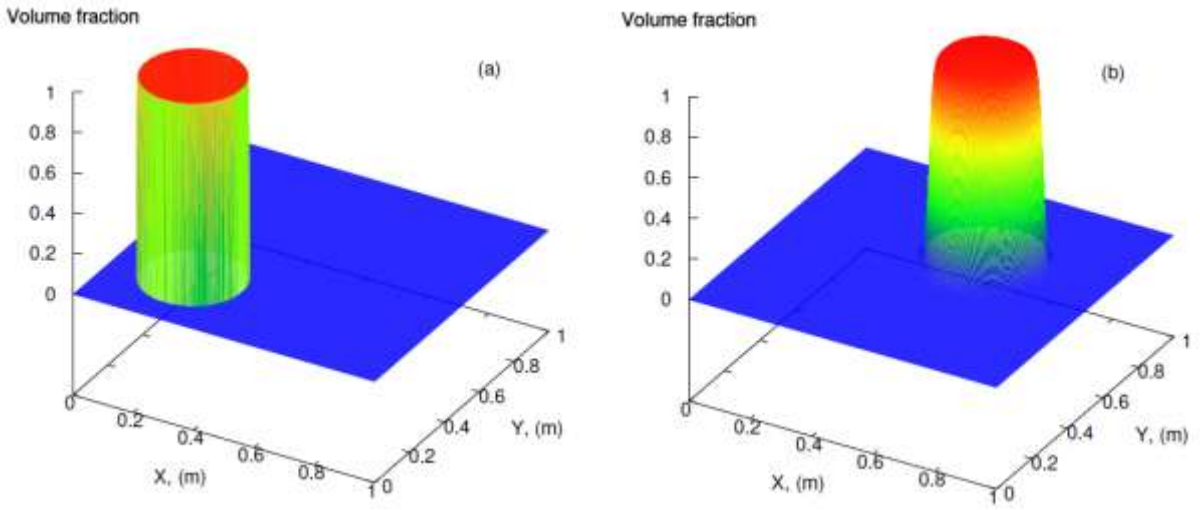

Fig. 3. Volume fraction surface plots (a) at time t = 0 s and (b) at time t = 0.36 s.

Underwater explosion

This test has been considered here to investigate the interaction between a strong shock wave and free material interface. The test is conducted in a square domain 1.2 m x 1.2 m as shown in Figure 4. A highly pressurised cylindrical air bubble with a radius of 0.1 m is located at (0.6, 0.6) m and a horizontal free air-water surface is located at 0.9 m. The initial conditions for the air bubble, water and air above the water are given in Table 4. All domain boundaries are set to be far field, i.e. extrapolation boundary condition, except at the bottom boundary which is set to be a solid wall with reflective boundary condition. Figure 5 shows the results of the simulations obtained using HLL Riemann solver with a mesh of 600 x 600 cells and a CFL number equal to 0.4. The results of the mixture density are displayed using an idealized Schlieren function at different times 0.0155, 0.031, 0.07, 0.146, 0.226 and 0.3 ms, respectively. The underwater explosion results in a strong shock wave propagating radially outward in the water. This is represented by the outer circle in Figure 5(a). At the same time, a strong rarefaction wave propagates inward in the air cylinder. This is represented by the inner circle in Figures 5(a-c). The material interface separating air cylinder and water is represented by the middle circle in Figures 5(a-c). When the shock wave strikes the horizontal free surface a rarefaction wave is generated. This wave propagates downward in the water as shown Figure 5(d). As soon as this rarefaction wave hits the air cylinder a compression wave is formed moving upward as shown in Figure 5(e). This results in an air cylinder changing its

shape to an oval. When the strong shock reaches the solid wall, at the bottom boundary of the computational domain, it is reflected upward as shown in Figure 5(f). A second shock wave is produced at the centre of the air cylinder which propagates outward as shown in Figures (e-f). As the time evolves the free surface moves upward as shown in Figures 5(d-f).

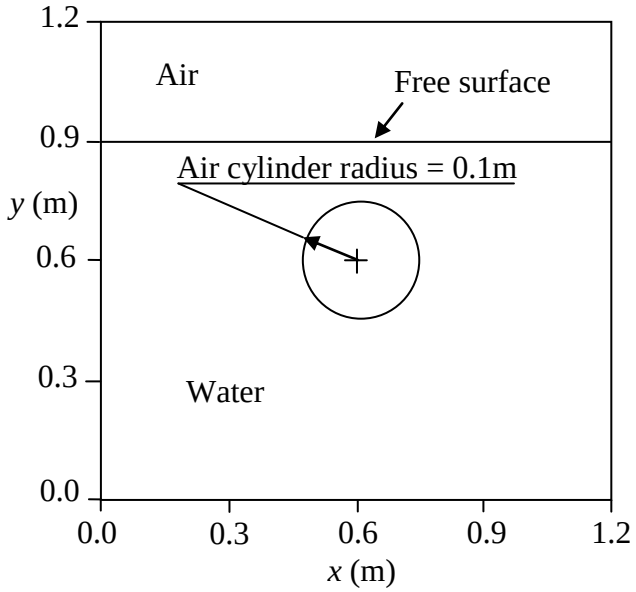

Fig. 4. Schematic diagram of the initial configuration of the underwater explosion test.

Table 4: Initial condition for underwater explosion problem.

Physical property	Air cylinder	Water	Air above water
Density, kg/m^3	1270	1000	1
Horizontal velocity, m/s	0	0	0
Vertical velocity, m/s	0	0	0
Pressure, Pa	9.12×10^8	1.1×10^5	1.1×10^5
Heat capacity ratio (γ)	1.4	4.4	1.4
Pressure constant (π)	0	6×10^8	0

Shock-bubble interaction

This test was earlier investigated experimentally by (Layes and Le Métayer, 2007). Figure 6 presents the computational domain and the initial configuration of the test involving the interaction of a shock wave with a helium bubble. The initial conditions for the helium bubble, air in pre shock chamber and air in high pressure chamber are presented in Table 5. The simulations are conducted using HLL Riemann solver, a mesh resolution of 900×240 and a CFL = 0.3. The shock wave propagates from right to left with a Mach number = 1.5 in the air and impacts the helium bubble. Figure 7 shows numerically obtained maps of the mixture density which were recorded at various moments of the simulation and post processed using the idealized Schlieren function. One can notice that as a consequence of the shock interaction with the helium bubble the gas bubble evolves generating two symmetric structures. The present results show a good approximation of the shape of the contours obtained in the experiment.

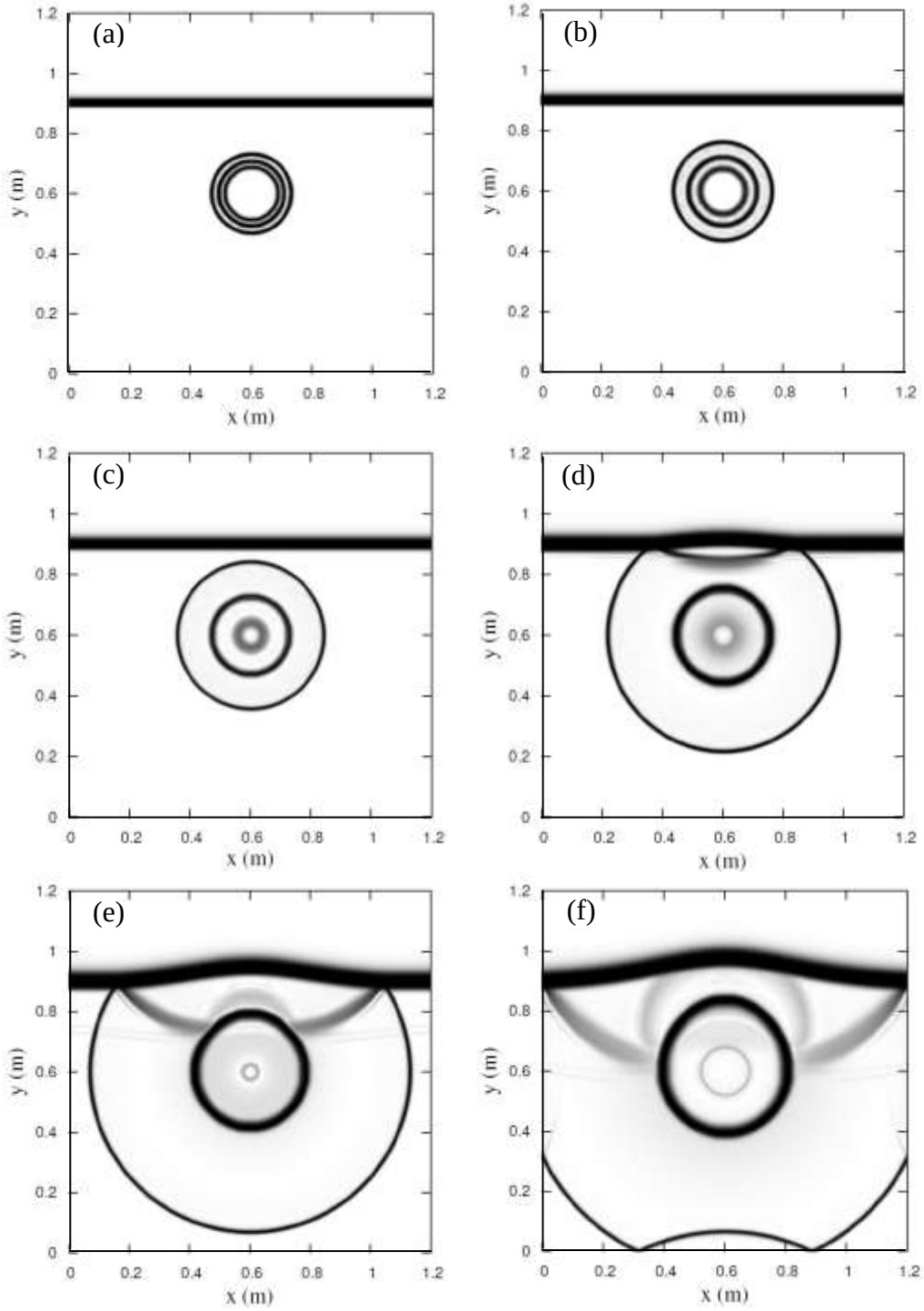

Fig. 5. The mixture density using idealised Schlieren function for underwater explosion at times 0.0155, 0.031, 0.07, 0.146, 0.226 and 0.3 ms.

CONCLUSIONS

Numerical simulations have been performed to capture the interface evolution in multi-component flows. The multiphase flow model applied was based on the concept of the diffuse interface method. The performance and accuracy of the developed numerical tools have been examined using a selection of test problems. The results show good agreement with idealized

analytical data for the cases where such data could be obtained from the relevant exact solution of the Riemann problem. The results also demonstrate physical trends when compared to available experimental data.

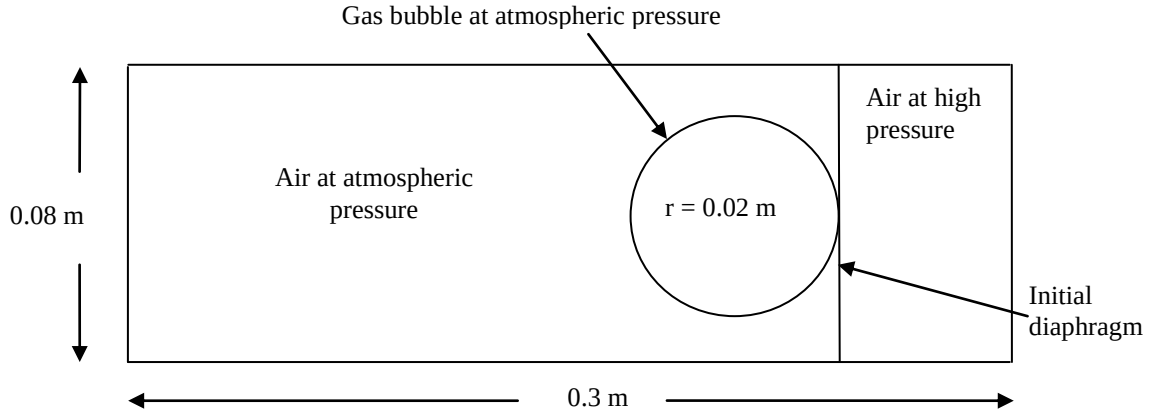

Fig. 6. Schematic diagram of the initial configuration of the shock-bubble interaction test

Table 5: Initial condition for shock-bubble interaction problem

Physical property	Air (pre-shock)	Helium bubble	Air (post-shock)
Density, kg/m^3	1.29	0.167	2.4021
Horizontal velocity, m/s	0	0	230.28
Vertical velocity, m/s	0	0	0
Pressure, Pa	1.01325×10^5	1.01325×10^5	2.4909×10^5
Heat capacity ratio (γ)	1.4	1.667	1.4
Pressure constant (π)	0	0	0

REFERENCES

Allaire, G., Clerc, S., Kokh, S., (2000): *A Five-equation Model for the Numerical Simulation of Interfaces in Two-phase Flows*, Comptes Rendus de l'Academie des Sciences - Series I: Mathematics, 331(12),pp.1017-1022.

Bates, K. R., Nikiforakis, N., Holder, D., (2007): *Richtmyer-Meshkov Instability Induced by the Interaction of a Shock Wave with a Rectangular Block of SF_6*, Physics of Fluids, 19, 036101

Baer, M. K., Nunziato, J. W. (1986): *A Two-phase Mixture Theory for the Deflagration-to-Detonation Transition (DDT) in Reactive Granular Materials*, International Journal of Multiphase Flow, Vol. 12, pp. 861-889

Ghangir, F., Nowakowski, A. F., (2012): *Computing the Evolution of Interfaces Using Multi-component Flow Equations*, Chapter 8 in *New Approaches in Modelling Multiphase Flows and Dispersion in Turbulence, Fractal Methods and Synthetic Turbulence*, Nicolleau, F.C.G.A., Cambon, C., Redondo, J.-M., Vassilicos, J.C., Reeks M. and Nowakowski, A.F. (Eds), Vol. 18, Springer, pp. 119-140, ISBN 978-94-007-2505-8.

Haas, J. F., Sturtevant, B., (1987): *Interaction of Weak Shock Waves with Cylindrical and Spherical Gas Inhomogeneities*, Journal of Fluid Mechanics, Vol. 181, pp.41-76.

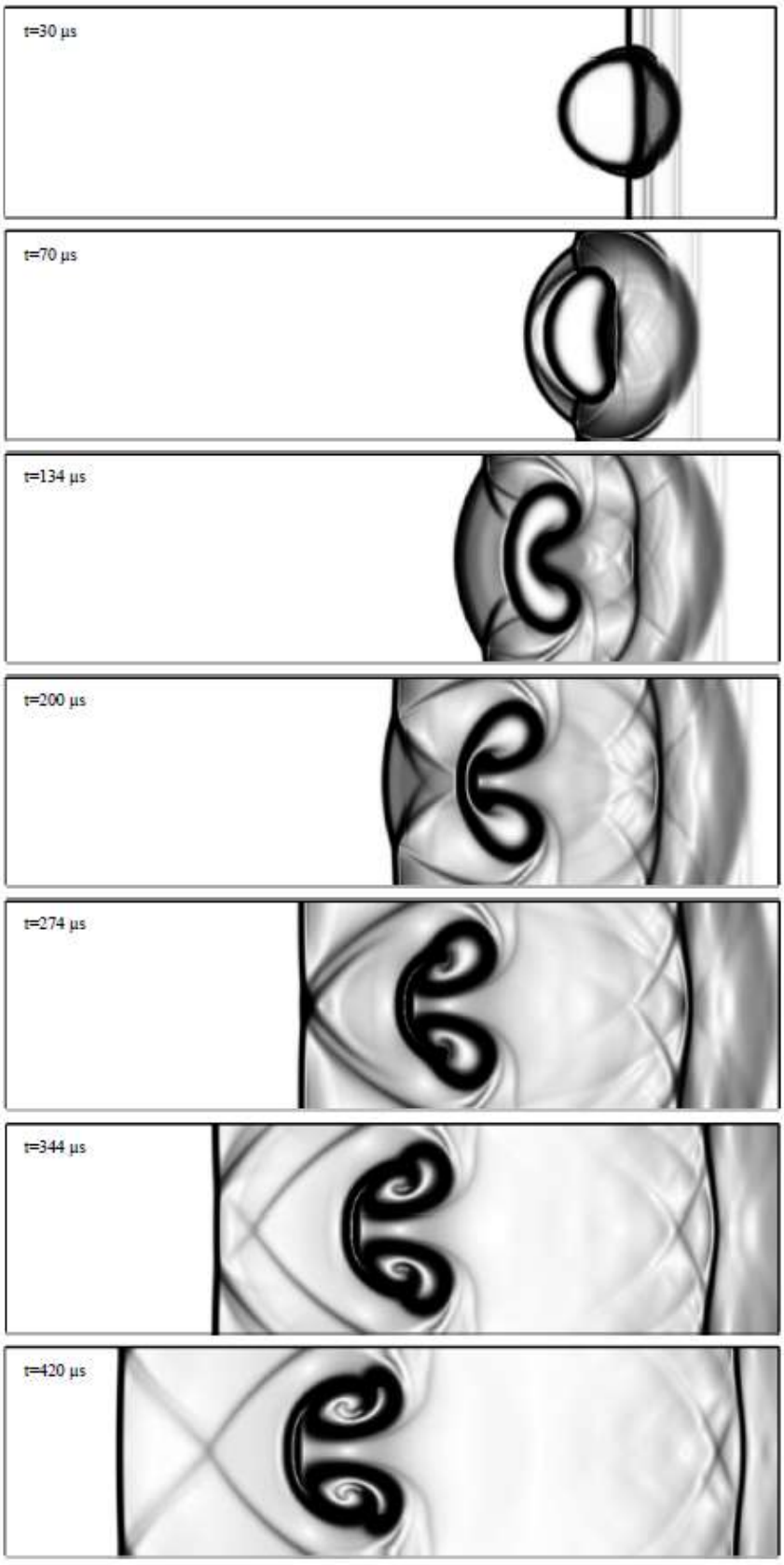

Fig. 7. The mixture density for the helium bubble-air constitution at times 30, 70, 134, 200, 274, 344 and 420 μs from top to bottom.

Hu, X. Y., Khoo, B. C., (2004): *An Interface Interaction Method for Compressible Multifluids*, Journal of Computational Physics, Vol. 198, pp.35–64.

Kapila, A., Menikoff, R., Bdzil, J., Son, S., Stewart, D., (2001): *Two-phase Modeling of Deflagration to Detonation Transition in Granular Materials: Reduced Equations*, Physics of Fluids, Vol.13, pp.3002-3024.

Lallemand, M. H., Chinnayya, A., Le Métayer, O., (2005): *Pressure relaxation procedures for multiphase compressible flows*, International Journal for Numerical Methods in Fluids 49 (1) 1-56.

Layes, G., Jourdan, G., Houas, L., (2003): *Distortion of a spherical gaseous inter-face accelerated by a plane shock wave*, Physical Review Letters 91(17), 174502.

Layes, G., Le Métayer, O., (2007): *Quantitative Numerical and Experimental Studies of the Shock Accelerated Heterogeneous Bubbles Motion*, Physics of Fluids, Vol. 19, 042105.

Murrone, A., Guillard, H., (2005): *A Five Equation Reduced Model for Compressible Two Phase Flow Problems*, Journal of Computational Physics 202(2), pp.664-698.

Nowakowski, A. F., Jolgam, S. A., Ballil, A. R., Nicolleau, F.C.G.A. (2011): *Simulation of Multiphase Flows with Strong Shocks and Density Variations*, Special issue of Proceedings of Applied Mathematics and Mechanics, Vol. 11, Issue 1, pp. 781-782

Saurel, R., Abgrall, R. (1999): *A Multiphase Godunov Method for Compressible Multi-fluid and Multiphase Flows*, Journal of Computational Physics, Vol. 150(2), pp.425-467.

Saurel, R., Lemetayer, O., (2001): *A Multiphase Model for Compressible Flows with Interfaces, Shocks, Detonation Waves and Cavitation*, Journal of Fluid Mechanics Vol.431, pp.239-271.

Saurel, R., Petitpas, F., Berry, R. A., (2009): *Simple and Efficient Relaxation Methods for Interfaces Separating Compressible Fluids, Cavitating Flows and Shocks in Multiphase Mixtures*, Journal of Computational Physics, Vol. 228, Issue 5, pp. 1678-1712

Shukla, R. K., Pantano, C., Freund, J. B., (2010): *An Interface Capturing Method for The Simulation of Multi-phase Compressible Flows*, Journal of Computational Physics, Vol. 229, pp.7411-7439.

Shyue, K. M., (1998): *An Efficient Shock-capturing Algorithm for Compressible Multi-component Problems*, Journal of Computational Physics, Vol.142, pp.208-242.

Strang, G. (1968): *On the Construction and Comparison of Difference Schemes*, SIAM J. Numer. Anal., 5:506-517.

Toro, E. (2009): *Riemann Solvers and Numerical Methods for Fluid Dynamics: A Practical Introduction*, Springer.

Zheng, H. W. and Shu, C. and Chew, Y. T., (2010): *A solution adaptive simulation of compressible multi-fluid flows with general equation of state*, International Journal for Numerical Methods in Fluids, Vol. 67, Number 5, pp. 616-637.